Rheology of living materials

Roxana Chotard-Ghodsnia, Claude Verdier

1

Rheology of living materials

R. Chotard-Ghodsnia

Laboratoire de Spectrométrie Physique, UJF-CNRS, UMR 5588
BP87, 140 avenue de la Physique
F-38402 Saint-Martin d'Hères, France

and
C. Verdier

Laboratoire de Spectrométrie Physique, UJF-CNRS, UMR 5588
BP87, 140 avenue de la Physique
F-38402 Saint-Martin d'Hères, France

Abstract.
In this chapter, the properties of biological materials are described both from a microscopic and a macroscopic point of view. Different techniques for measuring cell and tissue properties are described. Models are presented in the framework of continuum theories of viscoelasticity. Such models are used for characterizing experimental data. Finally, applications of such modeling are discussed in a few situations of interest.

1 Introduction

1.1 What is rheology ?

Rheology (in greek, rheos: to flow, –logy: the study of) is a pluridisciplinary science describing the flow properties of various materials, i.e. the

study of the stresses that are needed to produce certain strains or rate of strains within a given material. It consists of different approaches which are all needed to understand the complexity of fluids or materials possessing viscoelastic or viscoplastic properties. The main approaches are :

- Measurements of the rheological properties in simple flows (shear and elongation)
- Simultaneous description of the underlying microstructure as a function of deformation
- Constitutive modeling using generalized continuum or molecular models based on the previous observations
- Applications to real situations (complex flows and geometries)
- Numerical simulations when analytical works are not possible

Typical fluids or materials under investigation in the framework of rheology can be polymers (including polymer solutions, rubbers, polymer emulsions), suspensions of particules or deformable objects (e.g. blood cells), and other complex systems (foams, gels, tissues, etc.) as described by Larson [LAa].

1.2 Importance of rheology in the study of biological materials

Biological materials (see Textbook by Fung [FUa] or review paper by Verdier [VEa]) start at the cell level (order of a few microns) and can reach sizes up to the size of an assembly of cells or tissue (a few millimeters). Rheology is important for describing such materials since they are usually made of the above mentioned systems. The cell (Fig.1), to start with, possesses an elastic nucleus, a viscous or viscoplastic cytoplasm, and is surrounded by an elastic membrane made of a lipid bilayer, where adhesion proteins coexist [ALa].

An example of a biological fluid is blood, which is a suspension of proteins (i.e. Polymers) and cells (erythrocytes, as well as various white blood cells) inside a fluid (plasma). Another example is the one of a biological tissue. It contains an assembly of cells connected to each other by the extra-cellular matrix (ECM) and adhesion proteins. These complex systems lead to viscoelastic properties due to the presence of fluids (viscous effects), and the presence of elastic components (particles, inclusions with interfacial tensions, elastic membranes). Several rheological models can already predict such behaviors. The complexity of the biological tissue or fluid relies on the fact that such media are active, and can rearrange their microstructure to produce different local (or non local) properties or

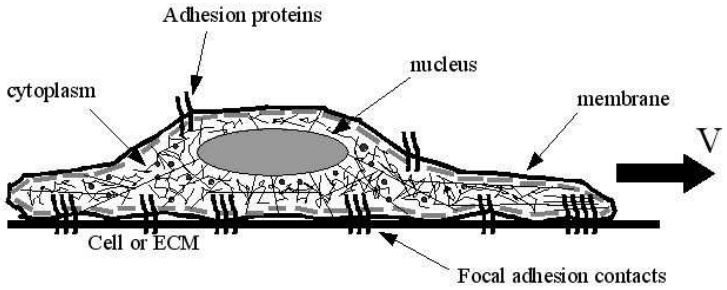

Figure 1: Sketch of a cell modifying its contacts and microrheology to undergo migration, at velocity V

stresses in order to resist, or to achieve a precise function, in other words, they are intelligent materials.

In this chapter, we will describe a few rheological models useful for modeling complex media. Then a brief description of biological media will be presented. Measuring techniques to investigate the properties of cells and tissues will then be explained. Finally, we will present a few examples of predictions achieved through rheological modeling.

2 Rheological models

In this section, a simple 1D viscoelastic model, the Maxwell model, and a viscoplastic 1D one, the Bingham model, are presented. These models are quite interesting to start with and can provide valuable information for the interpretation of simple experiments. Then a generalization of such models will be made in three dimensions.

2.1 One-dimensional models

The Maxwell fluid

We consider a simple viscoelastic 1D model, which is depicted in Fig. 2 where a spring (spring constant G) and dashpot (viscosity η) are assembled in series. The resulting stress, τ, is the same in the two elements whereas the deformation γ, is the sum of the deformations in each element. This leads to the following constitutive equation :

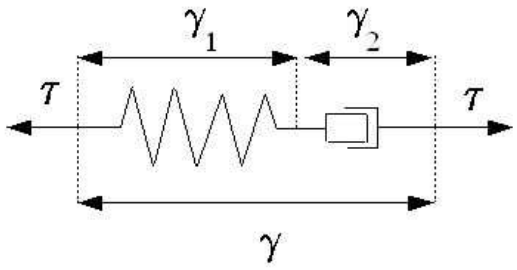

Figure 2: Schematic representation of the Maxwell element

$$\lambda\,\dot{\tau} + \tau = \eta\,\dot{\gamma} \tag{2.1}$$

where $\lambda = \frac{\eta}{G}$ is the relaxation time, and $\dot{\gamma}$ is the rate of deformation. This form is the differential form of the Maxwell model. It leads to a decrease in stress $\tau(t) = \tau_0\, exp\,(-\frac{t}{\lambda})$, when motion is stopped, where τ_0 is the initial stress.

Limiting cases of elastic and viscous materials can be recovered:

- When $t \ll \lambda$ (short times), $\tau = G\gamma \Rightarrow$ The material is elastic ($G = \frac{\eta}{\lambda}$).
- When $\lambda \ll t$ (long times), $\tau = \eta\dot{\gamma} \Rightarrow$ The material is Newtonian.

Equation (2.1) has an exact solution which is :

$$\tau(t) = \int_{-\infty}^{t} G\, e^{-\frac{(t-t')}{\lambda}}\, \dot{\gamma}(t')\, dt' \tag{2.2}$$

Relation (2.2) is the integral version of the Maxwell model. It has the advantage to show that the stress is a function of the history of deformation, and shows also that stress and rate of strain are related via this integral form with a Kernel $G(t) = G\, exp\,(-\frac{t}{\lambda})$. This function is called the relaxation function. Similarly, a relation between the strain $\gamma(t)$ and the stress $\tau(t)$ can be obtained in integral form through another Kernel $J(t) = \frac{1}{G} + \frac{t}{\eta}$ which is called the compliance.

Remark 2.1 *The other simple model considered in the literature is the Kelvin-Voigt model consisting of a spring and dashpot in parallel. This model exhibits a constitutive equation of the type* $\tau = G\,\gamma + \eta\,\dot{\gamma}$. *In this case* $G(t) = G$ *and* $J(t) = \frac{1}{G}(1 - exp\,(-\frac{t}{\lambda}))$, *where* λ *is defined similarly but is a retardation time.*

A generalization to multiple mode Maxwell models can easily be made through the use of the following distribution (G_i, λ_i) appearing in the relaxation function, corresponding to the use of several Maxwell elements in series:

$$G(t) = \sum_{i=1}^{n} G_i \, e^{-\frac{t}{\lambda_i}} \tag{2.3}$$

This is sometimes enough to obtain a good idea of the dynamic moduli, often used in oscillatory rheometry [BIc]. Otherwise, one may use a continuous distribution of relaxation times:

$$G(t) = \int_0^\infty \frac{H(\lambda)}{\lambda} \, exp\,(-\frac{t}{\lambda}) \, d\lambda \tag{2.4}$$

Such formulae have been used successfully for predicting the dynamic rheology of molten polymers, in particular Baumgaertel and Winter [BAc] who used two specific empirical formulae for $H(\lambda)$ for small times and long times.

The Bingham fluid

Bingham fluids are an example of the so–called viscoplastic materials. A Newtonian fluid can flow under the action of any stress but it is unlikely that a Bingham fluid will do the same. Indeed, it usually requires that a certain stress, i.e. the so–called "yield stress", is applied. For example, under the action of its weight alone, a fluid element might or might not flow. This relies on the fact that the typical stress (shear, elongation) dominates the effect of the Yield stress. Yield stresses are due to complex interactions taking place at the microscopic level, which link the material particles. A solution of F–actin (essential component of the cytoplasm), as an example, can flow only if the actin concentration is not too large. If it is large, then interactions between the actin proteins are such that temporary links exist throughout the fluid, showing the existence of a Yield effect.

The simplest 1D model (in the case of shear) is the Bingham fluid [MAa], given by :

$$\begin{aligned} &\tau \leq \tau_s \qquad \dot{\gamma} = 0 \quad \text{or} \quad \tau = G\,\gamma \\ &\tau \geq \tau_s \qquad \tau = \tau_s + \eta\,\dot{\gamma} \end{aligned} \tag{2.5}$$

This relation explains that a certain stress, τ_s, needs to be overwhelmed by the shear stress (τ) to achieve flow. Under this threshold, no flow is

obtained, but a simple elastic relation can be verified generally. Above this threshold, the material exhibits a Newtonian behavior with viscosity η. Other viscoplastic relations exist, like the Casson model (useful for describing the behavior of blood, at different hematocrit contents), or the Herschel-Bulkley model [MAa]. Finally, note that the cell cytoplasm may be modeled using the Bingham model or Herschel-Bulkley model, based on the constituents in presence. Another model introduced by He and Dembo [HEa], is the sol–gel model: it has been found to be successful to predict cell division. Sol-gel models can help predicting transitions from a liquid state ("sol") to a quasi–solid state ("gel") when a certain constituent's concentration is reached.

2.2 Three-dimensional models

To start with, we recall the principle relations used in classical fluid mechanics and elasticity, before presenting the 3D viscoelastic models. Let us define the total stress tensor $\underline{\underline{\mathbf{\Sigma}}}$ with an isotropic part, and an extra stress $\underline{\underline{\tau}}$:

$$\underline{\underline{\mathbf{\Sigma}}} = -p\,\underline{\underline{\mathbf{I}}} + \underline{\underline{\tau}} \tag{2.6}$$

where p is the pressure, and $\underline{\underline{\mathbf{I}}}$ is the identity tensor. To define constitutive equations and generalize the 1D ones in the previous section, we need to define laws valid for all observers (principle of material frame-indifference). Indeed, two observers in given reference frames should be able to measure the same material properties or laws. Consider a motion $\vec{\mathbf{x}} = \vec{\mathbf{x}}(\vec{\mathbf{X}}, \mathbf{t})$ and stress tensor $\underline{\underline{\mathbf{\Sigma}}} = \underline{\underline{\mathbf{\Sigma}}}(\vec{\mathbf{X}}, \mathbf{t})$. Another observer with clock $t^* = t - a$, in a frame defined by $\vec{\mathbf{x}}^* = \vec{\mathbf{x}}^*(\vec{\mathbf{X}}, \mathbf{t}^*) = \vec{\mathbf{c}}(\mathbf{t}) + \underline{\underline{\mathbf{Q}}}\,\vec{\mathbf{x}}(\vec{\mathbf{X}}, \mathbf{t})$, should observe a stress $\underline{\underline{\mathbf{\Sigma}}}^* = \underline{\underline{\mathbf{Q}}}(t)\,\underline{\underline{\mathbf{\Sigma}}}\,\underline{\underline{\mathbf{Q}^{\mathbf{T}}}}(t)$, following Malvern [MAd] for example. In the previous relations, a, $\vec{\mathbf{c}}$ and $\underline{\underline{\mathbf{Q}}}$ are respectively any constant, vector and orthogonal tensor. $\underline{\underline{\mathbf{\Sigma}}}$ is said to be frame–indifferent.

General fluids

For the classical Newtonian fluid, the extra stress is expressed in terms of $\underline{\underline{\mathbf{D}}}$, the symmetric part of the velocity gradient tensor, which is frame–indifferent. This defines the isotropic Newtonian fluid:

$$\underline{\underline{\mathbf{\Sigma}}} = -p\,\underline{\underline{\mathbf{I}}} + \lambda\, tr(\underline{\underline{\mathbf{D}}})\,\underline{\underline{\mathbf{I}}} + 2\eta\,\underline{\underline{\mathbf{D}}} \tag{2.7}$$

where η and λ are the viscosity and second viscosity coefficient respectively. For incompressible fluids, the equation simply reduces to $\underline{\underline{\mathbf{\Sigma}}} = -p\,\underline{\underline{\mathbf{I}}} + 2\eta\,\underline{\underline{\mathbf{D}}}$.

More general fluids can be defined, such as the Reiner-Rivlin fluid, where one makes use of the fact that an expansion of the stress in terms of the powers of $\underline{\underline{\mathbf{D}}}$ is also a good model and can be reduced to powers of $\underline{\underline{\mathbf{D}}}$ and $\underline{\underline{\mathbf{D}}}^2$ only.

$$\underline{\underline{\mathbf{\Sigma}}} = -\,p\,\underline{\underline{\mathbf{I}}} + \,2\,\eta\,\underline{\underline{\mathbf{D}}} + \,4\,\eta_2\,\underline{\underline{\mathbf{D}}}^2 \tag{2.8}$$

where η_2 is considered to be a second viscosity, but has different units ($Pa.s^2$). In equation (2.8), the constants η and η_2 depend on the invariants of $\underline{\underline{\mathbf{D}}}$, in particular II_D. Note that the first invariant I_D is 0 for incompressible materials. Equation (2.8), associated with the assumption that $\eta_2 = 0$, has been used extensively to predict the shear thinning (and thickening) behavior of polymer solutions and suspensions [MAa].

Elastic materials

Similarly to fluids, the constitutive equation of an isotropic elastic material gives the stress $\underline{\underline{\mathbf{\Sigma}}}$ in terms of the linear part of deformation $\underline{\underline{\epsilon}}$ (symmetric part of $\underline{\underline{\vec{grad}\,\vec{\mathbf{u}}}}$, where $\vec{\mathbf{u}} = \vec{\mathbf{x}} - \vec{\mathbf{X}}$ is the displacement between the initial and present position, in Lagrangian coordinates) :

$$\underline{\underline{\mathbf{\Sigma}}} = \lambda\, tr(\underline{\underline{\epsilon}})\,\underline{\underline{\mathbf{I}}} + 2\,\mu\,\underline{\underline{\epsilon}} \tag{2.9}$$

where λ and μ are the Lamé coefficients (in Pa). The generalization of this relation to large deformations is made possible through the use of the frame–indifferent strain tensor $\underline{\underline{\mathbf{B}}} = \underline{\underline{\mathbf{F}}}\,\underline{\underline{\mathbf{F}}}^T$, where $\underline{\underline{\mathbf{F}}}$ is the deformation gradient. Again, by assuming the stress to be a polynomial function of $\underline{\underline{\mathbf{B}}}$, and making use of the Cayley–Hamilton theorem, we obtain a relation for large deformations, the so–called Mooney–Rivlin model (MR):

$$\underline{\underline{\mathbf{\Sigma}}} = \alpha\,\underline{\underline{\mathbf{I}}} + 2\,C_1\,\underline{\underline{\mathbf{B}}} \,-\, 2\,C_2\,\underline{\underline{\mathbf{B}}}^{-1} \tag{2.10}$$

where C_1 and C_2 are constants in the MR model but may also be functions of the invariants of $\underline{\underline{\mathbf{B}}}$. α is a constant which needs, like a pressure, to be determined, for example through boundary conditions.

More generally, any function of the invariants of $\underline{\underline{\mathbf{B}}}$ can be used, via a strain energy function $W(I_B, II_B)$. Here, for an incompressible material $III_B = 1$. This defines a more general hyperelastic material:

$$\underline{\underline{\mathbf{\Sigma}}} = \alpha\,\underline{\underline{\mathbf{I}}} + \,2\,\frac{\partial W}{\partial I_B}\,\underline{\underline{\mathbf{B}}} \,-\, 2\,\frac{\partial W}{\partial II_B}\,\underline{\underline{\mathbf{B}}}^{-1} \tag{2.11}$$

Viscoelastic materials

If one wants to generalize the case of the Maxwell element in equation (2.1), it is natural to replace the 1D stress τ by the tensor $\underline{\underline{\tau}}$, then to replace $\dot{\gamma}$ by its tensor form $2\,\underline{\underline{\mathbf{D}}}$. Still one needs to be careful about the generalization of $\dot{\tau}$, because $\underline{\underline{\dot{\tau}}}$ is not frame–indifferent. In fact, there is a limited number of frame–indifferent derivatives [MAd], such as the following upper and lower convected derivatives given by, respectively:

$$\overset{\nabla}{\underline{\underline{\tau}}} = \underline{\underline{\dot{\tau}}} - \underline{\underline{\vec{grad}\vec{\mathbf{v}}}}\ \underline{\underline{\tau}} - \underline{\underline{\tau}}\ (\underline{\underline{\vec{grad}\vec{\mathbf{v}}}})^T \tag{2.12}$$

$$\overset{\triangle}{\underline{\underline{\tau}}} = \underline{\underline{\dot{\tau}}} + \underline{\underline{\tau}}\ \underline{\underline{\vec{grad}\vec{\mathbf{v}}}} + (\underline{\underline{\vec{grad}\vec{\mathbf{v}}}})^T\ \underline{\underline{\tau}} \tag{2.13}$$

The corotational derivative is also another one, $\overset{\circ}{\underline{\underline{\tau}}} = \frac{1}{2}\,(\overset{\nabla}{\underline{\underline{\tau}}} + \overset{\triangle}{\underline{\underline{\tau}}})$, as well as other linear combinations of the above two. Note that we are now using the extra stress $\underline{\tau}$.

Following this, we obtain the upper convected Maxwell model, as the generalized differential form of (2.1):

$$\lambda\,\overset{\nabla}{\underline{\underline{\tau}}} + \underline{\tau} = 2\,\eta\,\underline{\underline{\mathbf{D}}} \tag{2.14}$$

There is also an integral version of this equation:

$$\underline{\tau}(t) = \int_{-\infty}^{t} M(t-t')\,(\underline{\underline{\mathbf{B}}}(t,t') - \underline{\underline{\mathbf{I}}})\,dt' \tag{2.15}$$

where $M(t) = \frac{\eta}{\lambda^2}\,exp\,(-\frac{t}{\lambda}) = -\frac{dG}{dt}$, and $\underline{\underline{\mathbf{B}}}(t,t')$ is the relative deformation tensor. Formula (2.15) is called Lodge's formula and can include general functions $G(t)$, for example such as the ones in (2.3), or more generally decreasing convex functions which have a finite value for $G(0)$.

Finally, a generalization of Lodge's model, as well as ideas developed in the previous part on elasticity, in particular equation (2.11), lead to another more general form, known as the K–BKZ equation (factorized form):

$$\underline{\tau}(t) = \int_{-\infty}^{t} M(t-t')\,[2\,\frac{\partial W}{\partial I_B}(I_B, II_B)\ \underline{\underline{\mathbf{B}}}(t,t') - 2\,\frac{\partial W}{\partial II_B}(I_B, II_B)\,\underline{\underline{\mathbf{B}}}^{-1}(t,t')]\,dt' \tag{2.16}$$

This model has been used quite a lot for predicting the elongational properties of polymers or polymer solutions, and gives excellent agreement [WAa]. On the other hand, it is not so good for predicting shear data [BIc].

Viscoplastic models

The generalization of Equation (2.5) to a tensor form gives:

$$\begin{aligned} II_\tau \leq \tau_s \qquad & \underline{\underline{\mathbf{D}}} = \underline{\underline{\mathbf{0}}} \quad \text{or} \quad \underline{\underline{\tau}} = G\underline{\underline{\mathbf{B}}} \\ II_\tau \geq \tau_s \qquad & \underline{\underline{\tau}} = 2\,(\eta + \tfrac{\tau_s}{\sqrt{II_{2D}}})\,\underline{\underline{\mathbf{D}}} \end{aligned} \tag{2.17}$$

where $II_\tau = \frac{1}{2}(tr(\underline{\underline{\tau}})^2 - tr(\underline{\underline{\tau}}^2))$ is the second invariant of the extra stress tensor $\underline{\underline{\tau}}$. This way of defining the inequality implies that all components of the stress may contribute to overwhelm the Yield effect. Other possible models (Herschel–Bulkley, Papanastasiou, Casson [MAa]) can be used, in particular using the fact that the viscosity η in (2.17) may be taken to be a function of the invariants of $\underline{\underline{\mathbf{D}}}$, in particular II_D. As an example, models that characterize blood will be described in the part concerning rheological modeling of tissues and biofluids.

3 Biological materials

The response of a material to applied loads depends upon its internal constitution and interconnections of its microstructural components. Biological tissues are composed of the same basic constituents: cells and extracellular matrix.

3.1 Cells

Cells are the fundamental structural and functional unit of tissues and organs. It has been known over the last two decades that many cell types change their structure and function in response to changes in their mechanical environment. A typical cell consists of a cell membrane, a cytoplasm and a nucleus [ALa].

The cell membrane consists of a phospholipid bilayer with many embedded proteins that function as: channels, receptors for target molecules and anchoring sites.

The cytoplasm is a fluid containing the cytoskeleton and dispersed organelles.

The cytoskeleton is a network of protein filaments extending throughout the cytoplasm. The cytoskeleton provides the structural framework of the cell, determining the cell shape and the general organization of the

cytoplasm. The cytoskeleton is responsible for the movements of entire cells and for the intracellular transport. It is formed by three structural proteins: actin filaments, intermediate filaments and microtubules. Actin filaments are extensible and flexible (5-9 nm in diameter). Intermediate filaments are rope-like structures (10 nm in diameter). Microtubules are long cylinders (25 nm in diameter) with a higher bending stiffness than the other filaments. These three primary structural proteins perform their functions through interactions with accessory cytoskeletal proteins, such as actinin, myosin and talin.

The organelles play various roles. For example the Golgi apparatus plays a role in the synthesis of polysaccharides and in the transport of various macromolecules. The endoplasmic reticulum is the site for the synthesis of proteins and lipids.

The extracellular matrix consists of proteins (collagens, elastin, fibronectin, vitronectin, ...), glycosaminoglycans and water. Collagen, the most abundant protein in the body and a basic structural element for soft and hard tissues, and elastin, the most linearly elastic and chemically stable protein, are primary structural constituents of the extracellular matrix, from a mechanical point of view. The extracellular matrix has many functions. It serves as an active scaffold on which cells can adhere and migrate. It serves as an anchor for many substances (growth factors, inhibitors) and provides an aqueous environment for the diffusion of nutrients between the cell and the capillary network. It maintains the shape of a tissue giving it strength and mechanical integrity. To resume, the extracellular matrix controls cell shape, orientation, motion and function.

3.2 Tissues

A tissue is a group of cells that performs a similar function. There are four basic types of tissues in the human body: epithelium, connective tissue, muscle tissue and nervous tissue [FAb].

Epithelium is a tissue composed of a layer of cells. It can line internal (e.g. endothelium which lines the inside of blood vessels) or external (e.g. skin) free surfaces of the body. Functions of epithelial cells include secretion, absorption and protection.

Connective tissue is any type of biological tissue with extensive extracelllular matrix which holds everything together. There are several basic types:

- Bone: contains specialized cells, osteocytes, embedded in a mineralized extracellular matrix and functions for general support, protection of organs and movements. It is a relatively hard and light-weight composite material. It is formed mostly of calcium phosphate which has relatively high compressive strength through poor tensile strength.

While bone is essentially brittle, it has a degree of elasticity contributed by its organic components (mainly collagen).

- Loose connective tissue: holds organs in place and attaches epithelial tissue to other underlying tissues. It also surrounds blood vessels and nerves. Fibroblasts are widely dispersed in this tissue and secrete strong fibrous proteins (e.g. collagen and elastin) and proteoglycans as an extracellular matrix.

- Fibrous connective tissue: has a relatively high tensile strength due to a relatively high concentration of collagenous fibers. This tissue is primarily composed of polysaccharides, proteins and water and does not contain many living cells. Such a tissue forms ligaments and tendons.

- Cartilage: is a dense connective tissue primarily found in joints. It is composed of chondrocytes which are dispersed in a gel-like extracellular matrix mainly composed of chondroitin sulfate.

- Blood: is a circulating tissue composed of cells (hematies, leukocytes and platelets) and fluid plasma (its extracellular matrix). The main function of Blood is to supply nutrients (e.g. glucose, oxygen) and to remove waste products (e.g. carbon dioxyde). It also transports cells and different substances (hormones, lipids, amino acids) between tissues and organs.

- Adipose tissue: is an anatomical term for loose connective tissue composed of adipocytes. It provides cushioning, insulation and energy storage.

Muscle is a contractile form of tissue. Muscle contraction is used to move parts of the body and substances within the body. There are three types of muscles:

- Cardiac muscle.

- Skeletal muscle (or "volontary"): attached to the skeleton and used for movement.

- Smooth muscle (or "involontary"): found within intestines, throat and blood vessels.

The nervous tissue has the function of communication between parts of the body. It is composed of neurons, which transmit impulses, and the neuroglia, which assist the propagation of the nerve impulse and provides nutrients to the neurons.

4 Measurements of rheological properties of cells and tissues

4.1 Microrheology

Conventional rheological measurements are not always adapted to biological materials because they require large quantities of rare materials and provide an average measurement and do not allow for local measurements in inhomogeneous systems. Microrheological methods address this issue by probing the material on a micrometer length scale using microliter sample volumes. Two microrheological approches can be found in the litterature: active tests and passive test.

Active tests

In this class of microrheological measurements, the stress is locally applied to the material by active manipulation of the probe through the use of electric or magnetic fields or micromechanical forces. Then, the resultant strain is measured to obtain the local shear moduli. We will describe three active manipulation techniques in the following paragraphes.

Optical tweezers. Optical tweezers consist of a focused laser directed at a micrometer-scale dielectric object, such as beads or organelles, and used to control their position [ASa]. For typical object sizes (0.5-10μm in diameter) used, the force (limited to the pN range) is generated by the refraction of the laser within the bead coupled with the differences in photon density from the center to the edge of the beam. Very small objects do not trap well because the trapping force decreases with decreasing object volume. By moving the focused laser beam, the trapped particle is forced to move and applies a local stress to the sample. The resultant particle displacement reports strain from which rheological properties can be obtained. Elasticity measurements are possible by applying a constant force with the optical tweezers and measuring the resultant displacement of the particle. Membrane elastic modulus of red blood cells were measured using this approach [HEc]. Frequency-dependent rheological properties can be measured by oscillating the laser position with an external steerable mirror and measuring the amplitude of the bead motion and the phase shift with respect to the driving force. Microrheology of soft materials was studied using this approach [HOa].

Magnetic tweezers and magnetic twisting. Magnets are used to apply either a linear force (magnetic tweezers) or a twisting torque (magnetic twisting) to embedded magnetic particles. The resultant particle displacements measure the rheological response of the surrounding material. Particle selection is critical because its magnetic contents influence the applied force. Ferromagnetic beads can generally exert large forces but they retain a part of their magnetization each time they are exposed to a magnetic field. Paramagnetic beads are less susceptible to magnetization but they exert smaller forces (typically 10 pN to 10 nN). Videomicroscopy is used to detect the displacements of the particles under applied forces. The spatial resolution is typically in the range of 10-20 nm and the temporal range is 0.01-100 Hz. Three modes of operation are available: 1) a viscometry measurement by applying a constant force, 2) a creep response measurement by applying a pulse-like excitation: using this method Bausch et al. found linear three-phasic creep responses consisting of an elastic domain, a relaxation regime and a viscous flow behavior for different cell types [BAd, BAe], 3) a measurement of the viscoelastic moduli in response to an oscillatory stress: using this method Fabry et al. [FAa] suggested that cytoskeleton may behave like a soft glassy material [BOa, SOa], existing close to a glass transition, rather than like a gel.

Atomic force microscopy. The atomic force microscope [BIb] has been widely used to study the structure of soft biological materials, in addition to imaging information about the surface topology. A soft cantilever is pushed into the sample surface. The cantilever deflection is measured by a laser detection system (reflecting laser beam off the cantilever and position sensitive photodetector). Knowing the cantilever's spring constant, the cantilever deflection gives the force required to indent a surface and this has been used to measure the local elasticity and viscoelasticity of thin samples and living cells. For elasticity measurements [RAa, ROa], a modified Hertz model is used to describe the elastic deformation of the sample by relating the indentation and the loading force. Elastic mapping of cells was possible using this technique [AHa]. A common source of error for very thin or soft materials is the contribution of the elastic response of the underlying substrate, on which the sample is placed. This contribution is higher for higher forces and indentations and can be reduced by using a spherical tip. This increases the contact area and allows to apply the same stress to the sample with a smaller force [MAb].

For viscoelastic measurements, an oscillating cantilever tip is used [AHa, MAb, ALb, MAc]. A small amplitude (5-20 nm) sinusoidal signal is applied normal to the surface around the initial indentation position at frequencies ranging from 20 to 400 Hz. Using this test, Mahaffy et al. [MAc] characterized the lamellipodium of fibroblast cells and obtained a rubber plateau-like behavior. Smith et al. [SMa] characterized the microscale vis-

coelasticity of smooth muscle cells with AFM indentation modulation in their fibrous perinuclear region. They found that the complex shear modulus, measured in response to nanoscale oscillatory perturbations, exhibited soft-glassy rheology. The elastic (storage) modulus of these cells scaled as a weak power-law and their loss modulus scaled with the same power-law dependence on frequency.

Passive tests

In this class of microrheological measurements, the passive motion of the probes, due to thermal or Brownian fluctuations, is measured [MAe]. In this case, no external force is applied to the material. Phenomenologically, embedded probes exhibit larger motions when their local environments are less rigid or less viscous. Both the amplitude and the time scale are important for calculating the mechanical moduli. The mean squared displacement (MSD) of the probe's trajectory is measured over various lag-times to quantify the probe's amplitude of motions over different time scales. In purely viscous materials, MSDs of probes vary linearly with lag-times. In purely elastic materials, MSDs are constant regardless of lag-times. A viscoelastic material can be modeled as an elastic network that is viscously coupled to and embedded in an incompressible Newtonian fluid. A natural way to incorporate the elastic response is to generalize the standard Stokes-Einstein equation for a simple, purely viscous fluid with a complex shear modulus to materials that also have a real component of the shear modulus [MAf]:

$$\tilde{G}(s) = \frac{k_B T}{\pi a s < \Delta \tilde{r}^2(s) >} \tag{4.1}$$

where s is the complex Laplace frequency, k_B is the Boltzmann's constant, T is the absolute temperature, a is the radius of the probe and $< \Delta \tilde{r}^2(s) >$ is the unilateral Laplace transform of the two-dimensional MSD $< \Delta r^2(t) >$. To compare with bulk rheology measurements, $\tilde{G(s)}$ can be transformed into the Fourier domain to obtain the complex shear modulus $G^*(\omega)$.

For most soft materials, the temperature cannot be changed significantly. Thus, the upper limit of the measurable elastic modulus depends on both the size of the embedded probe and on our ability to resolve small particle displacements. The resolution of detecting particle centers depends on the particle tracking method and ranges from 1 to $10nm$. This allows measurements with micron-sized particles of materials with an elastic modulus of 10 to $500Pa$. This is smaller than the range accessible by active

tests but sufficient to study many soft materials. Moreover, passive measurements have the advantage of dealing with the linear viscoelastic regime because no external stress is applied.

To use the generalized Stokes-Einstein relation (4.1) to obtain macroscopic viscoelastic shear moduli of a material, the medium should be treated as a continuum material around the embedded particle. Thus, the size of the embedded particle must be larger than any structural length scales of the material. Moreover, this relation is valid for a large frequency range ($10Hz - 100kHz$) which is much higher than traditional methods where inertial effects become significant around $50Hz$. The MSD of embedded particles should be measured with a very good temporal and spatial resolution to take full advantage of the range of frequencies and complex moduli measurable in a passive microrheology test. The MSD can be obtained from methods that directly track the particle position as a function of time or from light-scattering experiments.

The rheological properties of living cells have been measured using particle tracking microrheology. Yamada et al. [YAa] showed that the cytoplasmic viscoelasticity of kidney epithelial cells varied within subcellular regions and was dynamic. At low frequencies, lamellar regions ($820 \pm 520\, dyne/cm^2$) were more rigid than viscoelastic perinuclear regions ($330 \pm 250\, dyne/cm^2$) of the cytoplasm, but the spectra converged at high frequencies ($> 1000\, rad/s$).

Finally, other groups have used improved particle–tracking methods: in particular, Crocker et al. [CRa] have developed a two–point microrheology technique, based on cross correlation of the motion of two particles. Tseng et al. [TSa], on the other hand, used multiple-particle-tracking microrheology to spatially map mechanical heterogeneities of living cells.

To resume, microrheological techniques allow to characterize complex materials on length scales much shorter than those measured with macroscopic techniques. In an incompressible homogenous material, the response of an individual probe due to an external force (active tests) or to thermal fluctuations (passive tests) is an image of the bulk viscoelastic properties of the surrounding medium. In heterogenous materials, the motion of individual probes gives the local properties of the material, while cross-correlated motion of the probes gives its bulk properties. Moreover, viscoelastic properties can be measured in a larger frequency range ($0.01Hz$ to $100kHz$) than in macroscopic measurements.

4.2 Macroscopic tests

There are different macroscopic tests that can be carried out with biological tissues. They will be classified here into two categories : the ones giving access to shear properties (transient assays, steady shear, oscillations) such as pure shear and compression, or the ones giving access to

tensile or elongational properties.

Shear

Classical definitions of shear experiments need to be given first. Usually, it is common to carry out experiments in a rotational rheometer, when dealing with biological fluids or materials. This instrument allows to have access to stresses (or torques) and strains while measuring strains and stresses respectively. The basic idea is that operating in a circular geometry allows to keep the fluid (material) in the same device, whereas capillary rheometry requires systems which push the fluid therefore they require a larger amount of material. Usual rotational rheometers include different geometries such as the plate–plate, cone–plate and Couette geometry (usually used for less viscous fluids). There is a different working formula for each one.

Transient motions. In classical rheometry, one applies a steady shear rate $\dot{\gamma}$ (in fact start–up from 0 to $\dot{\gamma}$) while the stress $\tau = \sigma_{12}$ is measured. Then the transient viscosity $\eta^+(t,\dot{\gamma})$, the first and second normal stress coefficients $\psi_1^+(t,\dot{\gamma})$ and $\psi_2^+(t,\dot{\gamma})$ can be determined :

$$\eta^+(t,\dot{\gamma}) = \frac{\sigma_{12}(t,\dot{\gamma})}{\dot{\gamma}} \tag{4.2}$$

$$\psi_1^+(t,\dot{\gamma}) = \frac{(\sigma_{11}-\sigma_{22})(t,\dot{\gamma})}{\dot{\gamma}} \tag{4.3}$$

$$\psi_2^+(t,\dot{\gamma}) = \frac{(\sigma_{22}-\sigma_{33})(t,\dot{\gamma})}{\dot{\gamma}} \tag{4.4}$$

They are named the viscosimetric functions. If these behaviors correspond to typical viscoelastic materials, one expects a rise of $\eta^+(t,\dot{\gamma})$, $\psi_1^+(t,\dot{\gamma})$, and $\psi_2^+(t,\dot{\gamma})$, until a plateau is reached. The limiting values will then be $\eta(\dot{\gamma})$, $\psi_1(\dot{\gamma})$, $\psi_2(\dot{\gamma})$. When elastic effects are important at high shear rates for example, there might be an overshoot in the time–evolution of the previous functions [BIc] until a steady state is found.

Steady–state functions. As previously discussed, the steady–state functions $\eta(\dot{\gamma})$, $\psi_1(\dot{\gamma})$, $\psi_2(\dot{\gamma})$ are the limits of the time–dependent functions as time becomes large. These limits are usually reached in times inversely proportional to the velocity of deformation (shear rate $\dot{\gamma}$ here). Materials or fluids with a decreasing $\eta(\dot{\gamma})$ are said to be shear–thinning whereas the opposite is the shear-thickening behavior, as observed for certain suspensions of particles. When the stress goes to a limit at small shear rates, the material exhibits a Yield stress as explained previously for Bingham fluids.

The first and second normal stress differences are quite important, since they are related to elastic effects, not usually encountered with Newtonian fluids. They correspond to the fact that the application of a shear in the 1–2 plane can given rise to normal stresses σ_{22} and σ_{33} in the other directions (rod–climbing effect, etc.).

Dynamic rheometry. This is the most common test used for characterizing biological materials, when large quantities of materials are available (collagen, actin solutions, etc.) and when such properties can be considered to be homogeneous, and not local. In shear, one applies a sinusoidal deformation $\gamma(t) = \gamma_0 sin(\omega t)$. The stress τ is assumed, to vary like $\tau(t) = \tau_0 sin(\omega t + \varphi)$. One of its components is in phase with γ (elastic response), while the other one varies like $\dot{\gamma}$ (viscous part). One defines respectively the elastic and viscous moduli G' et G". They are defined by $G'\,\gamma_0 = \tau_0\, cos\varphi$ and G" $\gamma_0 = \tau_0\, sin\varphi$. The loss angle, φ, is given by $tan\varphi = \frac{G"}{G'}$. In complex variables, the complex modulus G^* is: $G^* = G' + i\,G$" and the dynamic complex viscosity is $\eta^* = \frac{G^*}{i\omega} = \eta' - i\eta" = \frac{G"}{\omega} - i\frac{G'}{\omega}$. Moduli G' and G" are determined for small deformations (linear domain), i.e. the domain where they remain constant for small enough γ_0. An example of the dependence of G' and G" vs. frequency ω is given in Fig.3.

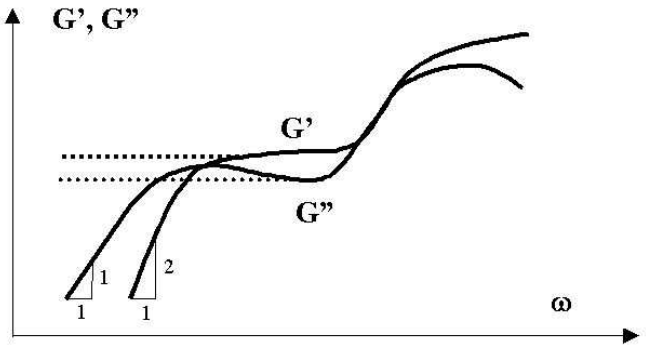

Figure 3: Dependence of G'(Pa) and G"(Pa) on frequency $\omega(rad/s)$. At low frequencies, the fluid exhibits Yield effects (dotted lines), such as in the case of concentrated actin solutions [SCa] or decreases with slopes 2 and 1 respectively, like in the limiting case of the Newtonian fluid (solid lines).

As can be seen, two different behaviors can be obtained :

- Newtonian behaviors at low rates: Case of usual fluids with respective slopes 2 and 1 for G' and G".
- Yield stress effects: G' and G" have a limiting value (fluid with a

yield stress).

At moderate frequency values, G' exhibits a plateau value usually (case of polymer solutions) and at high frequencies, G' and G" increase similarly as ω^n, where n is about $0.5 - 0.7$, until the solid–high frequency regime is obtained.

Remark 4.1 *The Maxwell model (Fig.2) has a complex modulus* $G^* = G\frac{i\omega\lambda}{1+i\omega\lambda}$ *therefore* $G'(\omega) = G\frac{\omega^2\lambda^2}{1+\omega^2\lambda^2}$ *and* $G"(\omega) = G\frac{\omega\lambda}{1+\omega^2\lambda^2}$. *This allows to recover the typical behavior at low frequencies corresponding to the slopes of* 2 *and* 1 *for* G' *and* $G"$.

Extension

The extensional properties of viscoelastic biological materials have been usually characterized using traction machines [FUa], or more subttle systems when biofluids are used. Usually constant rates of extension should be used, although this is rarely the case. In a constant stretching experiment at rate $\dot{\epsilon}$, the fluid element length increases exponentially, which is difficult to achieve. The elongational stresses of interest are combined to eliminate pressure effects in the form $\sigma_{11} - \sigma_{22}$, and the transient elongational viscosity is defined by:

$$\eta_E^+(t, \dot{\epsilon}) = \frac{\sigma_{11} - \sigma_{22}}{\dot{\epsilon}}(t, \dot{\epsilon}) \tag{4.5}$$

If formula (4.5) has a limit for infinite times, then the elongational viscosity $\eta_E(\dot{\epsilon})$ can be defined. This limit exists usually at small enough elongational rates $\dot{\epsilon} < \frac{1}{2\lambda}$ (λ is the relaxation time defined previously), but it happens (as in the Maxwell's fluid) that there is no limit above this value.

Typical instruments for obtaining constant stretch experiments are the traction experiment, the spinning fiber method, or the opposed jet method and four-roll mill apparatus for less viscous fluids [MAa].

Usually, the cases of biological materials under investigation has lead to results which give rise to hyperelasticity, as depicted by sharply increasing stress-strain curves, but there is always a small effect due to the rate of stretch [FUa] which is usually neglected, unlike with biofluids.

5 Applications of rheological models

5.1 Cells

In this section, a few examples of successful predictions of cell modeling corresponding to real situations are presented, in particular in the case of cell motion under flow, and in the case of cell migration.

Cell behavior under flow

Basic ideas. Red blood cells have a very precise size (diameter $8 - 10\mu m$) whereas Leukocytes are usually bigger (around $15\mu m$). Cells are able to travel through arteries or veins and also through small capillaries which are of the order a few μm. They must therefore possess very special rheological properties to achieve these features; sometimes they can also migrate through the endothelial barrier (case of leukocytes or cancer cells). Let us consider the case of a single cell travelling in a vessel, and assume that the plasma is Newtonian. When subjected to an applied pressure, it takes an equilibrium position depending on the viscosity ratio and on the Capillary number (ratio of viscous forces over surface effects). For leukocytes in capillaries for example, assuming the Reynolds number is small, and that the viscosity ratio is usually larger than 1, the cell will take an equilibrium position between the wall and the centerline, and its deformation will basically depend on the Capillary number [FUa].

To model a cell, several possibilities exist. The first authors to model cells used a membrane with a cortical tension surrounding a Newtonian fluid [YEa]. This model is already a good one for red blood cells. Membranes can also be considered to be linearly elastic or nonlinear elastic sheets [SKa] (deriving from a strain energy function). They usually have a large 2D–elastic modulus so that their surface is almost inextensible. They only exhibit a bending energy [HEb]. Other possibilities (droplet–like models) like a Newtonian fluid surrounded by a cortical layer [YEa] are also possible, and have proved to be efficient for describing micropipette experiments for example. Finally, viscoelastic cells with a cortical tension have been proposed recently [KHa], [VEb], and seem to be good candidates for describing cell behavior under flow.

Usually, due to the constraints, or simply to the fact that cells do not really travel in a linear fashion, they will eventually get close to the vascular wall and interact with it. This is studied next.

Modeling cell interactions. Cells are known to exhibit proteins (LFA–1, MAc–1, ICAM–1, etc.) on their surface, also named ligands (ICAM–1, VCAM–1, etc.). These ligands might interact with receptors present at the wall, on the endothelial lining. A simple reaction between a ligand (L) and a receptor (R) can give rise to a bond (L–R) according to:

$$L + R \rightleftharpoons L - R \tag{5.1}$$

Assume that N_L^0 and N_R^0 are the initial concentrations of ligands and receptors respectively, and that N is the number of bonds formed, then the rate–equation for N is:

$$\frac{dN}{dt} = k_f(N_L^0 - N)(N_R^0 - N) - k_r N \tag{5.2}$$

This is called a kinetics equation for cell–mediated adhesion. The solution of this equation starts at an initial prescribed value and then decreases until a plateau is reached. This model (microscopic) can be coupled with usual macroscopic equations describing the cell behavior [DEb], therefore it is a way to couple the microscopic and macroscopic descriptions. Indeed, the forward and backward constants k_f and k_r are respectively known through:

$$k_f = k_f^0 \, exp\,[-\frac{\sigma_{ts}(x_m - \lambda)^2}{2k_B T}] \tag{5.3}$$

$$k_r = k_r^0 \, exp\,[\frac{(\sigma - \sigma_{ts})(x_m - \lambda)^2}{2k_B T}] \tag{5.4}$$

where k_f^0 and k_r^0 are constants, x_m is the bond length, λ the equilibrium length, k_B is the Boltzmann constant and T is temperature. σ and σ_{ts} (transition state) are the spring constants.

Then the force within a bond is simply given by $f_B = \sigma(x_m - \lambda)$, and finally the macroscopic force F_B is equal to the single force times the bond density N: $F_B = N f_B$ [DEb]. Other simple models may use a force F_B which is attractive and derive from a simple attractive potential [VEb].

Models combining cell viscoelasticity and interactions.

There is a limited number of studies devoted to the motion of cells close to a wall. The most interesting ones are studies by Dembo et al. [DEb], N'Dry et al. [NDa], Liu et al. [LIa], Jadhav et al. [JAa], Khismatullin et al. [KHa] or Verdier et al. [VEb]. The first studies are 2D analyses of the motion of cells close to walls using kinetic models described previously. Let us discuss the cases of the works of Khismatullin et al. [KHa] and Jadhav et al. [JAa]. dealing with 3D problems.

Khismatullin et al. [KHa] used a nonlinear viscoelastic model for the cell description. This model is a Giesekus model which is the same as the one in Eq.(2.14), except that the nonlinear term $\kappa \underline{\underline{\tau}}^2$ on the left hand side has been added. Note that this type of nonlinear equation is useful for predicting shear transient motions during start–up. The originality of the work is also that a composite cell is considered. Indeed, the cell consists of a viscoelastic nucleus and a viscoelastic cytoplasm. A kinetic law of

attachment–detachment is used as previously described. Finally, cortical tensions are imposed at the boundaries. The problem of the motion of a cell close to a wall (with receptors) is considered in the presence of microvili. Deformability of the cell is calculated under physiological conditions (shear stresses of $0.8 - 4Pa$), as well as inclination angle, flow field, contact times and microvili number of attachments. Typically, cells are deformed quite a lot and exhibit a very small contact area.

Let us now compare this analysis with a quite different model [JAa], where viscoelasticity is introduced through the combined effects of a non-linear elastic membrane with a Newtonian cytoplasm. The same kinetics of bonds formation is used but a stochastic process is used to model receptor–ligand interactions. For example, the probability of bond formation $P = 1 - exp(-k_{on}\Delta t)$, where k_{on} is a formation constant, is introduced and compared with a random number between 0 and 1. If it is larger, the bond will form, otherwise not. Differences with the previous model are obtained. Indeed, the cells are less deformed and exhibitit a round shape, but adhere very strongly and form a much larger contact area, increasing with decreasing membrane elasticity. This can be understood since the stronger the membrane, the more spherical the cell, therefore the smaller number of bonds are formed.

To compare the models, one needs to compute a Capillary number $C_a = \frac{\eta V}{\sigma}$ in the first case [KHa] (η is the viscosity of the carrying fluid and V a typical stream velocity), and $Ca = \frac{\eta V}{Eh}$ in the second one [JAa], because the elastic component acting against the flow to stabilize the cell shape is either the cortical tension σ or the elastic 2D modulus Eh (E is the elastic modulus and h the membrane thickness). We find that the case considered by Khismatullin et al. [KHa] leads to very large Capillary numbers, thus to large deformations whereas the model of Jadhav et al. [JAa] has capillary numbers of order 1, thus smaller deformations. Still, the flow field plays a role, as well as the model used and the other parameters. More studies are still needed to understand such problems better; they might be very important for understanding cancer cell extravasation, especially since cancer cells are considered to be less rigid as compared to other cells.

Cell migration

Principle of migration. Cell migration is a complex mechanism, which involves both the adhesive properties but also the rheological properties of the cell, as depicted in Fig.1. Under chemotaxis or haptotaxis, a cell can polarize and develop a lamellipodium which extends far to the front [COb], in the case of a fibroblast on a rigid surface. Inside the cell, changes

in the local actin concentration can generate changes in the microrheological properties, allowing the cell to deform and move. Actin filaments can form cross–links at the front (like in a gel), whereas they become less densely packed (sol) at the uropod (tail), in order to preserve the total actin concentration. In order for the cell to move, it requires to generate traction forces to pull itself forward. These forces are generated by focal adhesion plaques, such as integrin clusters. Some cells can migrate very fast like the neutrophils of the immune system (mm/hour) whereas other cells, such as cancer cells, reach velocities of only a few tenth of $\mu m/hour$. There is a complex machinery involving Actin binding proteins (ABP) together with myosin to form actin units. Other disassembly proteins are also needed to break actin units. Integrins bind to the cytoskeleton which is made of parallel bundles of actin filaments, thus creating a reinforced structure, which allows the cell to generate tractions forces. Such traction forces can be measured on deformable substrates in the case of fibroblasts for example [DEa]. Other methods also exist based on wrinkle patterns on deformable substrates as well [BUa] and provide interesting information in the case of keratocytes.

Models of cell migration. In order to migrate efficiently, a cell must develop strong traction forces, but they should not be too large, otherwise they will be difficult to break at the rear. Indeed there is an optimal velocity of migration [PAa] depending on the typical bond forces or cell–substrate affinity. One way to model adhesion is through a distribution of bonds, as seen previously. This idea comes from observations (RICM) of adhering cells showing unattached cell parts. The model of Dickinson and Tranquillo [DIa] assumes such a distribution of receptor-ligand bonds. Adhesion gradients can also be considered which influence cell motility. A stochastic model is assumed to show how migration is affected by the forces and the distribution of ligands on the cell. Adhesion receptors undergo rapid binding, and this results in a time–dependent motion. Mean speed, persistence time, and random motility coefficients can then be obtained. A bell-shape curve is finally obtained showing a maximum in velocity as a function of the adhesion concentration factor, as shown experimentally [PAa].

Another approach by DiMilla et al. [DIb] includes cell polarization, cytoskeleton force generation, and dynamic adhesion to create cell movement. A model for cell viscoelastic properties (1D) is also included. Similar effects for the velocity of migration as a function of force are obtained, but further effects such as force, cell rheology as well as receptor–ligand dynamics can be added. The maximum in the speed of migration is related to the balance between cell contractile force and adhesiveness.

Cancer cell migration. Cancer cell migration is different from the previous cells studied (fibroblasts, leukocytes). Friedl and coworkers [FRa]

have shown that tumor cells develop migrating cell clusters. They also seem to develop stronger interactions (and pulling forces) and are more polarized (direction). Most cancer cells are usually bigger and slower than migrating leukocytes. They are also capable of reorganizing the extra-cellular matrix (ECM) easily. Therefore, cancer cell migration is still hard to model and requires more experimental data.

5.2 Tissues

Biological tissues are complex structures subjected to a number of external stimuli (e.g. mechanical forces, electrical signals and heat). The structure of these tissues determines their response to the stimuli. In addition, cells within the tissues can sense the stimuli and adapt or change the tissue matrix structure. Biological tissues differ in many ways from typical engineering materials. They are extremely heterogenous within a single body and between individuals. They have always hierarchical structures with many different scales. And they are able to change their structure in response to external stimuli.

In this section, a few examples of connective tissue modeling such as blood and soft tissues under physiological loads are presented.

Blood

Blood is a circulating tissue. It is a complex fluid composed of Red Blood Cells (RBC or erythrocytes), White Blood Cells (WBC or leukocytes) and platelets suspending in plasma (an aqueous solution of electrolytes and proteins such as fibrinogen and albumin). Plasma is the extracellular matrix of blood cells). Blood cells volumic concentration (hematocrit) is about 38-45% corresponding to $5.10^6/mm^3$ of RBC, $5.10^3/mm^3$ of WBC and $3.10^5/mm^3$ of platelets. Plasma behaves like a Newtonian fluid of 1.2 mPa.s viscosity at $37°C$. The whole blood behaves like a non-Newtonian fluid. Its viscosity varies with the hematocrit, with the temperature and with the disease state [CHa].

When looking at blood flow in large vessels, it can be considered as a homogenous fluid. This can be analyzed using a Couette-flow viscometer where the width of the flow channel is much larger than the diameter of blood cells. Using Couette-flow viscometry, Cokelet et al. [COa] found that blood has a finite yield stress in shear. For a small shear rate ($\dot{\gamma} < 10s^{-1}$) and for hematocrit less than 40%, their data is approximately described by Casson's Law [CAa]:

$$\sqrt{\tau} = \sqrt{\tau_s} + \sqrt{\eta\dot{\gamma}} \tag{5.5}$$

where τ is the shear stress, $\dot{\gamma}$ the shear rate, τ_s is the yield stress in shear ($\approx 5.10^{-3}Pa$) and η is a constant. At high shear rates (about $100s^{-1}$), the whole blood behaves like a Newtonian fluid with a constant viscosity ($4-5mPa.s$). The whole blood flow in a cylindrical tube follows a plug flow profile [FUa]. This behavior can be explained by the fact that human RBCs form aggregates (known as rouleaux) which are more important under low shear rates. When the shear rate tends to zero the whole blood becomes like a big aggregate with a solid-like behavior (a viscoplastic behavior as described in §2.1). When the shear rate increases, the aggregates tend to break and the viscosity of blood decreases. For further increase in shear rate, RBCs become elongated and align with flow streamlines [GOa] inducing a very low viscosity ($3 - 4mPa.s$) for such a concentrated suspension.

When looking at blood flow in capillaries, it can be considered as a nonhomogenous fluid of at least two phases: blood cells and plasma. Indeed in capillaries, whose diameter is in the range of blood cells diameter ($4 - 10\mu m$), blood cells have to squeeze and arrange themselves in a single file [FUa]. Thus, mechanical properties of RBCs play a predominant role in the microcirculation. These cells are nucleus-free deformable liquid capsules enclosed by a nearly incompressible membrane which exibits elastic response to shearing and bending deformation. As an application of rheological measurements to determine RBCs mechanical properties, we can refer to the work of Drochon et al. [DRa]. They measured the rheological properties of a dilute suspension of RBCs and interpreted their experimental data based on a microrheological model, proposed by Barthes-Bièsel et al. [BAa]. This model illustrated the effect of interfacial elasticity on capsule deformation and on the rheology of dilute suspensions for small deformations. Thus, Drochon et al. determined the average deformability of a RBC population in terms of the mean value of the membrane shear elastic modulus.

Soft tissues

Most of biological tissues exhibit a time- and history- dependent stress-strain behavior that is a characteristic property of viscoelastic materials. Viscoelastic models for soft tissues can be divided into two groups: microstructural and rheological models.

Microstructural models are based on mechanical behavior of the constituents of the tissue. The mechanical response of the components are generalized to produce a description of the gross mechanical behavior of the tissue. For example, Lanir introduced a microstructural model of lung tissue [LAa]. He considered lung tissue as a cluster of a very large number

of closely packed airsacks (alveoli) of irregular polyhedron shape, bounded by the alveolar wall membrane. Lanir employed a stochastic approach to tissue's structure in which the predominant structural parameter is the density distribution function of membrane's orientation in space. Based on this model, the behavior of alveolar membrane and its liquid interface was related to general constitutive properties of lung tissue.

Another microstructural 2D model of lung tissue consisted of a sheet of randomly aligned fibers of various orientations embedded in a viscous liquid ground substance [BAb]. The fibers orientations constantly change due to thermal motion. When the sheet is stretched, the fibers align in the direction of strain and there is a net transfer of momentum between the fibers and the ground substance, due to the constant thermal motion of the fibers. This model also predicts that any stress generated within the tissue will decay asymptotically to zero as the fibers reorient.

Microstructural models were applied to other tissues. Guilak and Mow [GUa] modeled the articular cartilage based on a biphasic theory in which the tissue is treated as a hydrated soft material consisting of two mechanically interacting phases: 1) a porous, permeable, hyperelastic, composite solid phase composed of collagen, proteoglycans and chondrocytes; and 2) a viscous fluid phase, which is predominantly water and electrolytes. Both phases are intrinsically incompressible and diffusive drag forces between the two phases give rise to the viscoelastic behavior of the tissue. Such models are well suited to study the connection between the structure and the mechanical properties (stress, strain, fluid flow and pressurization).

Tensegrity models have been developped [FUb] based on the ideas of deformable structures (i.e. civil engineering) made of sticks and strings in tension or compression. They can be applied to cells [INa, INb], since the cell cytoskeleton can be depicted as an assembly of rods and springs (various cytoskeleton filaments). Similar ideas have been developped at a higher scale, by considering homogenization methods in the case of cardiomyocytes, assumed to form discrete lattices [CAb] of bars linked together. When the components are elastic, one can recover an elastic constitutive model, also hyperelasticity can be obtained.

Rheological models describe the gross mechanical behavior of the tissue in the simplest possible terms. Sanjeevi et al. [SAa] proposed a 1D–rheological model of viscoelastic behavior for collagen fibers. The quasilinear viscoelastic models (see for example Eq.(2.2)) have been useful to describe various tissues such as the heart muscle [PIa, HUa] and the cervical spine [MYa]. Bilston et al. [BIa] developped a constitutive model which accurately reproduces the strain-rate dependence of brain tissue and its linear stress-strain response in shear.

On the other hand, DeHoff [DEa] described the nonlinear behavior of soft tissues by adapting a continuum-based formulation previously used

to characterize polymers. Phan-Thien et al. [PHa] also used a nonlinear Maxwell model to predict the behavior of kidney under large-amplitude oscillatory squeezing flow. They added a nonlinear stress–dependent viscosity in front of $\underline{\underline{\mathbf{D}}}$ in Eq.(2.14). Nassiri et al. [NAa] developped a multi-mode upper convected Maxwell (see §2) model with variable viscosities and time constants for viscoelastic response, coupled to a hyperelastic response (see Eq.(2.11)). In their model, the sum of the elastic and the viscoelastic contributions were modified by a nonlinear damping function to control the non-linearity of stress-strain profiles: 1) In the limit of small strain (0.2%), the damping function reduced to unity and their model reduced to a multi-mode Maxwell model with shear-rate dependent viscosities, 2) In high strain rate loading, this model gave a rubber-like response. Their model predicted well the rheological properties of the kidney cortex under strain sweep, small amplitude oscillatory motion (dynamic testing), stress relaxation and constant shear rate (viscometry) tests. They showed that this tissue was highly shear thinning, and at higher strain amplitudes this phenomenon was more significant. The damping function was strain dependent and could be determined to match well various nonlinear features of the shear tests.

6 Conclusions

In this chapter, we have made an attempt to investigate the rheological properties of biological systems in a non exhaustive manner. There are at the moment good methods for characterizing tissues and fluids, but also cellular elements. Although these techniques are very promising, there is still a lack of characterizations of tissues or cells, coupled with microscopic observations, in particular the ones based on the use of fluorescence.

Some of these experimental procedures have been correlated successfully with existing models, which have already been developped in the field of classical rheology. It has also been shown that cell-cell interactions are very important when modeling cell or tissue behavior.

What are still missing today are actual models including the active response of the tissues or cells, which can in return induce changes to the cell cytoskeleton or membrane. Some progress has been done recently but there is a need for taking into account signalisation and its effects on the rheological properties, in other words understanding mechanotransduction.

Acknowledgements

This work has been made possible thanks to two European networks (HPRCT–2000–00105 and MRTN–CT–2004–503661) devoted to cancer modeling.

7 References

[AHa] A-Hassan, E., Heinz, W.F., Antonik, M.D., D'Costa, N.P., Nageswaran, S., Schoenenberger, C. and Hoh, J.H., Relative microelastic mapping of living cells by atomic force microscopy, *Biophys. J.*, **74** (1998), 1564–1578.

[ALa] Alberts, B., Bray, D., Lewis, J., Raff, M., Roberts, K. and Watson, J.D. **Molecular biology of the cell, 3rd edition**, Garland Publishing, New-York (1994).

[ALb] Alcaraz, J., Buscemi, L., Grabulosa, M., Trepat, X., Fabry, B., Farre, R. and Navajas, D., Microrheology of human lung epithelial cells measured by atomic force microscopy, *Biophys. J.*, **84** (2003), 2071–2079.

[ASa] Ashkin, A., Forces of a single-beam gradient laser trap on a dielectric sphere in the ray optics regime, *Biophys. J.*, **67** (1992), 569–589.

[BAa] Barthès-Biesel, D. and Rallison, J.M., The time dependent deformation of a capsule freely suspended in a linear shear flow, *J. Fluid Mech.*, **113** (1981), 251.

[BAb] Bates, J.H.T., A micromechanical model of lung tissue rheology, *Ann. Biomed. Eng.*, **26** (1998), 679–687.

[BAc] Baumgaertel, M. and Winter H.H., Determination of discrete relaxation and retardation time spectra from dynamic mechanical data, *Rheol. Acta*, **28** (1989), 511–519.

[BAd] Bausch, A.R., Ziemann, F., Boulbitch, A.A., Jacobson, K., and Sackmann, E., Local measurements of viscoelastic parameters of adherent cell surfaces by magnetic bead microrheometry, *Biophys. J.*, **75** (1998), 2038–2049.

[BAe] Bausch, A.R., Moller, W., and Sackmann, E., Measurement of local viscoelasticity and forces in living cells by magnetic tweezers, *Biophys. J.*, **76** (1999), 573–579.

[BIa] Bilston, L.E., Liu, Z., and Phan-Thien, N., Linear viscoelastic properties of bovine brain tissue in shear. *Biorheology*, **34** (1997), 377–385.

[BIb] Bining, G., Quate, C.F. and Gerber, C., Atomic force microscope, *Phys. Rev. Lett.*, **56** (1986), 930–933.

[BIc] Bird, R.B., Armstrong, R.C., and Hassager, 0., **Dynamics of Polymeric Liquids. Fluid Mechanics, Vol. I**, Wiley Interscience, New-York (1987).

[BOa] Bouchaud, J.–P., Weak ergodicity–breaking and aging in disordered systems, *J. Phys. I. France*, **2** (1992), 1705–1713.

[BUa] Burton, K., Park, J.H. and Taylor, D.L., Keratocytes generate traction forces in two phases, *Molecular Biol. of the Cell*, **10** (1999), 3745–3769.

[CAa] Casson, M., A flow equation for pigment-oil suspensions of the printing ink type, in: Mills, C.C., ed., **Rheology of disperse systems**, Pergamon, Oxford (1959).

[CAb] Caillerie, D., Mourad, A. and Raoult, A., Cell–to–muscle homogeneization. Application to a constitutive law for the myocardium, *Math. Model. Numer. Anal.*, **37** (2003), 681–698.

[CHa] Chien, S., Shear dependence of effective cell volume as a determinant of blood viscosity, *Science*, **168** (1970), 977–979.

[COa] Cokelet, G.R., Merrill, E.W., Gilliand, E.R., Shin, H., Britten, A. and Wells, R.E., The rheology of human blood measurement near and at zero shear rate, *Trans. Soc. Rheol.*, **7** (1963), 303–317.

[COb] Condeelis, J., Life at the leading edge: the formation of cell protrusions, *Ann. Rev. Cell Biol.*, **9** (1993), 411–444.

[CRa] Crocker, J.C., Valentine, M.T., Weeks, E.R., Gisler, T., Kaplan, P.D., Yodh, A.G. and Weitz, D.A., Two–point Microrheology of inhomogeneous materials *Phys. Rev. Lett.*, **85** (2000), 888–891.

[DEa] Dehoff, P.H. On the nonlinear viscoelastic behavior of soft biological tissues. *J. Biomech.*, **11** (1978), 35–40.

[DEb] Dembo, M. and Wang, Y.-L., Stresses at the cell-substrate interface during locomotion of fibroblasts, *Biophys. J.*, **76** (1999), 2307–2316.

[DEc] Dembo, M., Torney, D.C., Saxman, K. and Hammer, D., The reaction–limited kinetics of membrane to surface adhesion and detachment, *Proc. R. Soc. Lond. B*, **234** (1988), 55–83.

[DIa] Dickinson, R.B. and Tranquillo, R.T., A stochastic model for adhesion-mediated cell random motility and haptotaxis, *J. Math. Biol.*, **31** (1993), 563–600.

[DIb] DiMilla, P.A., Barbee, K. and Lauffenburger, D.A., Mathematical model for the effects of adhesion and mechanics on cell migration speed. *Biophys. J.*, **60** (1991), 15–37.

[DRa] Drochon, A., Barthès-Biesel, D., Lacombe, C. and Lelièvre, J.C., Determination of the red blood cell apparent membrane elastic modulus from viscometric measurements, *J. Biomech. Eng.*, **112** (1990), 241–249.

[FAa] Fabry, B., Maksym, G.N., Butler, J.P., Glogauer, M., Navajas, D. and Fredberg, J.J., Scaling the microrheology of living cells, *Phys. Rev. Lett.*, **87** (2001), 148102:1–4.

[FAb] Fawcett, D. W., **Bloom and Fawcett: a textbook of histology**, W. B. Saunders, 11th edn. Philadelphia (1986).

[FRa] Friedl, P., Brocker, E.B. and Zanker, K.S., Integrins, cell matrix interactions and cell migration strategies: fundamental differences in leukocytes and tumor cells. *Cell Adhes. Commun.*, **6** (1998), 225–236.

[FUa] Fung, Y.C., **Biomechanics. Mechanical properties of living tissues**, Springer–Verlag, New-York (1993).

[FUb] Fuller, R.B., Tensegrity, *Portfolio Artnews Annual*, **4** (1961), 112–127.

[GOa] Goldsmith, H.L., The microrheology of human erythrocyte suspensions, in: Becker, E. and Mikhailov, G.K., eds., **Theoretical and applied mechanics, Proc. 13th IUTAM Congress**, Springer, New York (1972).

[GUa] Guilak, F. and Mow, V.C., The mechanical environment of the chondrocyte: a biphasic finite element model of cell-matrix interactions in articular cartilage. *J. Biomech.*, **33** (2000), 1663–1673.

[HEa] He, X. and Dembo, M., A dynamic model of cell division, in: Alt, W., Deutsch, A. and Dunn, G. eds, **Mechanics of cell and tissue motion**, (1997), 55–66.

[HEb] Helfrich, W., Elastic properties of lipid bilayer: theory and experiments, *Z. Naturforsch*, **C28** (1973), 693–703.

[HEc] Hénon, S., Lenormand, G., Richert, A. and Gallet, F., A new determination of the shear modulus of the human erythrocyte membrane using optical tweezers, *Biophys. J.*, **76** (1999), 1145–1151.

[HOa] Hough, L.A. and Ou-Yang, H.D., A new probe for mechanical testing of nanostructures in soft materials, *J. Nanoparticle Res.*, **1** (1999), 495–499.

[HUa] Huyghe, J.M., Van Campen, D.H., Arts, T. and Heethar, R.M., The constitutive behaviour of passive heart muscle tissue: a quasi–linear viscoelastic formulation, *J. Biomech.*, **24** (1991), 841–849.

[INa] Ingber, D.E., Cellular tensegrity: defining the rules of biological design that govern the cytoskeleton. *J. Cell Sci.*, **104** (1993), 613–627.

[INb] Ingber, D.E., Heidemann, S.R., Lamoureux, P. and Buxbaum, R.E., Opposing views on tensegrity as a structural framework for understanding cell mechanics, *J. Appl. Physiol.*, **89** (2000), 1663–1678.

[JAa] Jadhav, S., Eggleton, C.D. and Konstantopoulos, K., A 3–D computational model predicts that cell deformation affects selectin–mediated leukocyte rolling, *Biophys. J.*, **88** (2005), 96–104.

[JOa] Johnson, G.A., Livesay, G.A., Woo, S.L.Y. and Rajagopal, K.R., A single integral finite strain viscoelastic model of ligaments tendons, *J. Biomech. Eng.*, **118** (1996), 221–226.

[KHa] Khismatullin, D.B. and Truskey, G.A., A 3D numerical study of the effect of channel height on leukocyte deformation and adhesion in parallel-plate flow chambers, *Microvasc. Res.*, **68** (2004), 188–202.

[LAa] Lanir, Y., Constitutive equations for the lung tissue, *J. Biomech. Eng.*, **105** (1983), 374–380.

[LAb] Larson, R.G., **The structure and rheology of complex fluids**, Oxford Univesity Press, New-York (1999).

[LIa] Liu, X.H. and Wang, X., The deformation of an adherent leukocyte under steady flow: a numerical study, *J. Biomechanics*, **37** (2004), 1079–1085.

[MAa] Macosko, C.W., **Rheology, principles, Measurements and Applications**, Wiley-VCH, New-York (1994).

[MAb] Mahaffy, R.E., Shih, C.K., MacKintosh, F.C. , and Käs, J., Scanning probe-based frequency-dependent microrheology of polymer gels and biological cells, *Phys. Rev. Lett.*, **85** (2000), 880–883.

[MAc] Mahaffy, R. E., Park, S., Gerde, E., Käs, J. and Shih, C.K., Quantitative analysis of the viscoelastic properties of thin regions of fibroblasts using atomic force microscopy, *Biophys. J.*, **86** (2004), 1777–1793.

[MAd] Malvern, L.E., **Introduction to the mechanics of a continuum medium**, Prentice Hall (1969).

[MAe] Mason, T.G., Ganesan, K., Van Zanten, J.H., Wirtz, D. and Kuo, S.C., Particle tracking microrheology, *Phys. Rev. Lett.*, **79** (1997), 3282–3285.

[MAf] Mason, T.G. and Weitz, D.A., Optical measurements of frequency-dependent linear viscoelastic moduli of complex fluids, *Phys. Rev. Lett.*, **74** (1995), 1250–1253.

[MYa] Myers, B.S., MacElhaney, J.H. and Doherty, B.J., The viscoelastic responses of the human cervical spine in torsion: Experimental

limitations of quasi-linear theory and a method for reducing these effects, *J. Biomech.*, **24** (1991), 811–817.

[NAa] Nasseri, S., Bilston, L.E. and Phan-Thien, N., Viscoelastic properties of pig kidney in shear, experimental results and modelling. *Rheol. Acta*, **41** (2002), 180–192.

[NDa] N'Dry, N.A., Shyy W. and Tran–Son–Tay, R., Computational modeling of cell adhesion and movement using a continuum–kinetics approach, *Biophys. J.*, **85** (2003), 2273–2286.

[PHa] Phan-Thien, N., Nasseri, S. and Bilston, L.E., Oscillatory squeezing flow of a biological material. *Rheol. Acta*, **39** (2000), 409–417.

[PIa] Pinto, and Fung, Y.C., Mechanical properties of the heart muscle in the passive state, *J. Biomech.*, **6** (1973), 597–606.

[PAa] Palececk, S.P., Loftus, J.C., Ginsberg, M.H., Lauffenburger, D.A. and Horwitz, A.F., Integrin-ligand binding properties govern cell migration speed through cell-substratum adhesiveness, *Nature*, **385** (1997), 537–540.

[RAa] Radmacher, M., Fritz, M., Kacher, C.M., Cleveland J.P., and Hansma, P.K., Measuring the viscoelastic properties of human platelets with the atomic force microscope, *Biophys. J.*, **70** (1996), 556–567.

[ROa] Rotsch, C., Jacobson, K. and Radmacher, M., Dimensional and mechanical dynamics of active and stable edges in motile fibroblasts investigated by using atomic force microscopy. *Proc. Natl. Acad. Sci. USA*, **96** (1999), 921–926.

[SAa] Sanjeevi, R., A viscoelastic model for the mechanical properties of biological materials, *J. Biomech.*, **15** (1982), 107–109.

[SCa] Schmidt, C., Hinner, B., and Sackmann, E., Microrheometry underestimates the viscoelastic moduli in measurements on F-actin solutions compared to macrorheometry, *Phys. Rev. Letters*, **61** (2000), 5646–5653.

[SHa] Shoemaker, P.A., Schneider, D., Lee, M.C. and Fung, Y.C., A constitutive model for two dimensional soft tissues and its application to experimental data, *J. Biomech.*, **19** (1986), 695–702.

[SKa] Skalak, R., Modeling the mechanical behavior of blood cells, *Biorheology*, **10** (1973), 229–238.

[SMa] Smith, B.A., Tolloczko, B., Martin, J.G., and Grütter, P., Probing the viscoelastic behavior of cultured airway smooth muscle cells with atomic force microscopy: stiffening induced by contractile agonist, *Biophys. J.*, **88** (2005), 2994–3007.

[SOa] Sollich, P., Lequeux, F., Hébraud, P. and Cates, M.E., Rheology of soft glassy materials, *Phys. Rev. Lett.*, **78** (1997), 2020–2023.

[STa] Stossel, T., On the crawling of animal cells, *Science*, **260** (1993), 1086–1094.

[TSa] Tseng, Y., Kole, T.P. and Wirtz, D., Micromechanical mapping of live cells by multiple-particle-tracking microrheology, *Biophys. J.*, **83** (2002), 3162–3176.

[VEa] Verdier, C., Review: Rheological properties of living materials. From cells to tissues, *J. Theor. Medicine*, **5** (2003), 67–91.

[VEb] Verdier, C., Jin, Q., Leyrat, A., Chotard-Ghodsnia, R. and Duperray, A., Modeling the rolling and deformation of a circulating cell adhering on an adhesive wall under flow, *Arch. Physiol. Biochem.*, **111** (2003), 14–14.

[WAa] Wagner, M.H., A constitutive analysis of extensional flows of polyisobutylene, *J. Rheol.*, **34** (1990), 943–958.

[YAa] Yamada, S., Wirtz, D. and Kuo, S.C., Mechanics of living cells measured by laser tracking microrheology, *Biophys. J.*, **78** (2000), 1736–1747.

[YEa] Yeung, A. and Evans, E., Cortical shell-liquid core model for passive flow of liquid-like spherical cells in micropipettes, *Biophys. J.*, **56** (1989), 139–149.